Journal of Zhejiang University SCIENCE A
ISSN 1673-565X (Print); ISSN 1862-1775 (Online)
www.zju.edu.cn/jzus; www.springerlink.com
E-mail: jzus@zju.edu.cn

Column envelope meshing pair and its design method for single screw compressors*

Wei-feng WU†, Quan-ke FENG

(*School of Energy and Power Engineering, Xi'an Jiaotong University, Xi'an 710049, China*)

†E-mail: wwf.jt@163.com

Received Mar. 1, 2008; Revision accepted June 17, 2008; Crosschecked Oct. 29, 2008

Abstract: A single screw compressor (SSC) is an important component found in many refrigeration systems. However, the durability is not so good because of the friction between its meshing pair. Therefore the column envelope meshing pair was proposed to prolong the operating life of SSCs, although it has not been applied to commercial refrigeration systems. To accelerate the industrial application, a mathematical model for analyzing the column envelope meshing pair is established based on the geometry and kinematics. Equations giving the flanks of column envelope grooves are obtained, and teeth flank meshing with the groove is designed. Results show that this model could be applicable in the design of the column envelope type SSC.

Key words: Column envelope, Single screw compressor (SSC), Meshing pair, design, Mathematical model
doi:10.1631/jzus.A0820146 **Document code:** A **CLC number:** TH455

INTRODUCTION

Single screw compressors (SSCs) (Zimmern *et al*., 1972), developed by Zimmern in the 1960s, are widely used in refrigeration, air/gas compression and chemical engineering systems (Wu and Tao, 2006). The structure of a typical SSC is shown in Fig.1. Essentially, a screw rotor meshes symmetrically with two star-wheels to double the swept volume and balance the radial thrust on the screw rotor (Zimmern *et al*., 1972), and their angular velocities, ω, have a relation as follows:

$$p=\frac{\omega_b}{\omega_a}=\frac{\phi_b}{\phi_a}=\frac{n_a}{n_b}=\frac{11}{6}, \tag{1}$$

where n is the teeth number; ϕ is the rotational angle as shown in Fig.2; subscripts 'a' and 'b' denote the star-wheel tooth and the screw rotor groove. In this article the teeth number ratio, p=11/6 is selected.

This ratio gives 12 gas packets per unit revolution of the rotor compared with 1 gas packet per unit crank revolution in a conventional reciprocating compressor, which reduces pressure pulsations in the discharge flow. The performance of an SSC is thus superior to that of a single piston design (Bein, 1991). And the performance of an SSC is superior to that of a twin screw compressor for its balanced radial thrust on the rotor (Zhang, 2007).

However, the discharge capacity of a newly produced SSC decreases sharply several hundred hours after operation (Zimmern *et al*., 1972) although the performance is good during the first operation. This behavior is un-doubtly attributed to rapid wear of the star-wheel teeth flank meshing with the screw grooves in the compressor (Zimmern, 2000). The use of high wear-resistance material helps to prolong the life of SSCs, but it does not solve the basic problem related to the operational life. We need to meet the challenge of developing a suitable structure profile for reducing friction between the two components of the meshing pair (Zimmern, 1990; Wu and Tao, 2005). The original type of meshing pair in an SSC is a straight line envelope meshing pair (LEMP). The contact line between the star-wheel tooth flank and

* Project (No. 2008AA05Z203) supported by the Hi-Tech Research & Development (863) Program of China

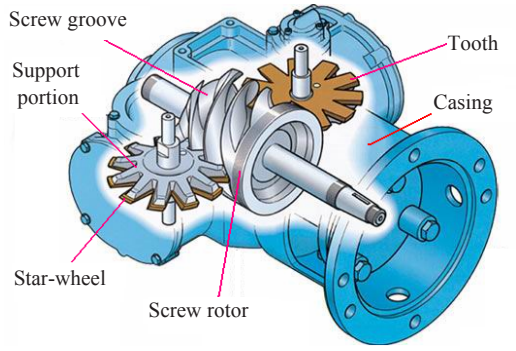

Fig.1 Basic components of a typical single screw compressor

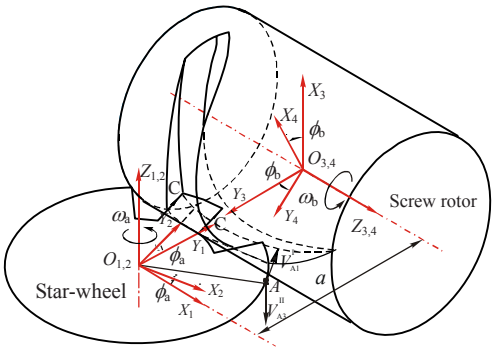

Fig.2 Schematic diagram of geometric and kinematic relations between the tooth and the groove

the screw rotor is fixed on the star-wheel tooth flank, and thus wear is progressive. Zimmern (1976) developed the column (frustum) envelope meshing pair (CEMP), which was expected to have good wear-resistance (Boblitt, 1987). And this type of meshing pair was modified by Jensen (1998; 2000) and Wu *et al.*(2007) to improve its machinability. However, little attention has been paid to the mathematical model of the CEMP (Yang, 2006; Yang and Liang, 2007; Zhang *et al*., 2006), although a mathematical model for the LEMP of an SSC was presented by Yang (2002).

This paper presents the mathematical model for designing the CEMP in the SSC.

MATHEMATICAL MODEL FOR THE CEMP

The basic idea for deriving the mathematical model is to extend the straight line of the LEMP to the column surface, and the groove flank is designed to be meshed smoothly with the column surface.

Coordinate systems

Four right-handed Cartesian coordinates are introduced (Jin and Tang, 1985) according to the geometric and kinematic relations between the tooth and the groove. As indicated in Fig.2, S_1 (X_1, Y_1, Z_1) and S_3 (X_3, Y_3, Z_3) coordinates are used for expressing the starting positions of the star-wheel and the rotor and thus are stationary; the origin O_1 is chosen at the center of the star-wheel; Z_1-axis is in the direction of the axis of the star-wheel; and Z_3-axis is on the axis of the screw rotor. The coordinates S_2 (X_2, Y_2, Z_2) and S_4 (X_4, Y_4, Z_4) are used for describing the rotation of the star-wheel and the screw rotor around the Z_1- and Z_3-axes.

Meshing between the tooth flank and the groove flank

The groove flank is an envelope of the tooth flank, which is a part of the envelope column surface as shown in Fig.3 (the cross section of the C-C in Fig.2).

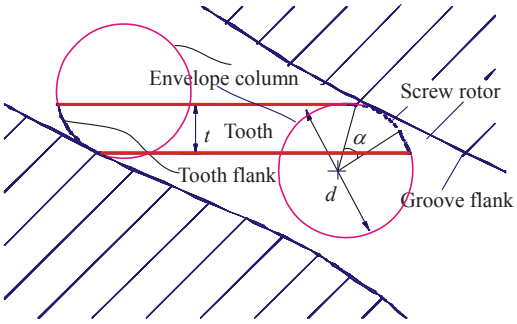

Fig.3 Cross section of the CEMP

The tooth flank and the groove flank must be moved with relative velocity in which each velocity should be tangential, i.e., relative velocity is tangential to the moving surfaces at the contact point. And thus the relative velocity of the surfaces at the contact points must be orthogonal to its normal vector (Kang *et al*., 1996; Liu *et al*., 2000; Richmond, 1996) shown as follows:

$$\boldsymbol{v}\cdot\boldsymbol{n}=0, \tag{2}$$

where $\boldsymbol{n}$ represents the normal vector of the column surface, and $\boldsymbol{v}$ is the relative velocity between the column surface and the groove flank.

An envelope column representing the tooth flank is fixed in the coordinate S_2 as shown in Fig.4, and the axis of the column is set normal to the Z_2-axis. In Fig.4, the coordinates L, K, and M denote the position of the envelope column denoted by "i" in the coordinate S_2; u is the height of point B on the envelope column; β is the inclinational angle of the envelope column, and its sign is determined by spiral right rules; θ is the circumferential angle of point B and is defined as the mesh angle. So the position of point B is

$$\boldsymbol{b}_2=\begin{bmatrix}x_2 & y_2 & z_2\end{bmatrix}^{\mathrm{T}}, \tag{3}$$

where

$$\begin{cases}x_2=L-u\sin\beta+\dfrac{d}{2}\cos\theta\cos\beta,\\ y_2=K+u\cos\beta+\dfrac{d}{2}\cos\theta\sin\beta,\\ z_2=M+\dfrac{d}{2}\sin\theta,\\ 0\le\theta<2\pi,\ \ 0\le u\le H,\end{cases}$$

where d is the diameter of the column; subscript '2' denotes the vector or the variable evaluated in the coordinate S_2. Assume that point B is a contact point when the coordinate S_2 rotates by ϕ_a. So the normal vector and the relative velocity of the column surface at point B should obey Eq.(2).

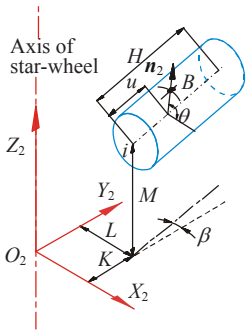

Fig.4 Column surface in coordinate S_2

The normal vector $\boldsymbol{n}$ can be given in the coordinate S_3 as follows:

$$\boldsymbol{n}_3=\left[-\cos\theta\cos(\beta+\phi_a),\ \sin\theta,\ -\cos\theta\sin(\beta+\phi_a)\right]^{\mathrm{T}}. \tag{4}$$

According to the kinematics between the star-wheel and the screw rotor, the relative velocity at point B is the difference between velocities of the star-wheel and the screw rotor at point B. Thus, the relative velocity at point B could be given in the coordinate S_3 by Eq.(5):

$$\begin{aligned}\boldsymbol{v}_3=\boldsymbol{v}_3^{\mathrm{a}}-\boldsymbol{v}_3^{\mathrm{b}}=\omega_a\big[&y_2\sin\phi_a-x_2\cos\phi_a-pz_2,\\ &p(a-y_2\cos\phi_a-x_2\sin\phi_a),\ y_2\cos\phi_a+x_2\sin\phi_a\big]^{\mathrm{T}}.\end{aligned} \tag{5}$$

The condition that the tooth flank and the groove flank should be meshed can be obtained by substituting Eqs.(3)~(5) into Eq.(2) and expressed as follows:

$$E(u,\phi_a)\cos\theta-F(u,\phi_a)\sin\theta=0, \tag{6}$$

where

$$\begin{cases}E(u,\phi_a)=L\sin\beta-K\cos\beta+pM\sin(\beta+\phi_a)-u,\\ F(u,\phi_a)=p\left[K\cos\phi_a+L\sin\phi_a+u\cos(\beta+\phi_a)-a\right].\end{cases}$$

The mesh angle θ can be derived from Eq.(6):

$$\theta(u,\phi_a)=\arctan\left[\frac{E(u,\phi_a)}{F(u,\phi_a)}\right], \tag{7}$$

or

$$\theta(u,\phi_a)=\pi+\arctan\left[\frac{E(u,\phi_a)}{F(u,\phi_a)}\right], \tag{8}$$

Eq.(7) and Eq.(8) are valid when the groove flank meshes with the tooth on its right and left flanks, respectively. Finally, the equation giving the surface of the groove flanks can be derived by substituting Eq.(7) or (8) into Eq.(3) and transformed from the coordinates S_2 to S_4, expressed as

$$\begin{aligned}&\boldsymbol{\varphi}(u,\phi_a,\phi_b,\theta)\\ &=\left[\chi(u,\phi_a,\phi_b,\theta)\quad\eta(u,\phi_a,\phi_b,\theta)\quad\xi(u,\phi_a,\phi_b,\theta)\right]^{\mathrm{T}},\end{aligned} \tag{9}$$

where

$$\begin{aligned}&\chi(u,\phi_a,\phi_b,\theta)\\ &=\left(L-u\sin\beta+\frac{d}{2}\cos\theta\cos\beta\right)\cos\phi_a\sin\phi_b\\ &\quad+\left(M+\frac{d}{2}\sin\theta\right)\cos\phi_b+a\sin\phi_b\\ &\quad-\left(K+u\cos\beta+\frac{d}{2}\cos\theta\sin\beta\right)\sin\phi_a\sin\phi_b,\end{aligned}$$

$$\eta(u,\phi_a,\phi_b,\theta)$$
$$=\left(L-u\sin\beta+\frac{d}{2}\cos\theta\cos\beta\right)\cos\phi_a\cos\phi_b$$
$$-\left(M+\frac{d}{2}\sin\theta\right)\sin\phi_b+a\cos\phi_b$$
$$-\left(K+u\cos\beta+\frac{d}{2}\cos\theta\sin\beta\right)\sin\phi_a\cos\phi_b,$$
$$\xi(u,\phi_a,\phi_b,\theta)$$
$$=\left(L-u\sin\beta+\frac{d}{2}\cos\theta\cos\beta\right)\sin\phi_a$$
$$+\left(K+u\cos\beta+\frac{d}{2}\cos\theta\sin\beta\right)\cos\phi_a.$$

From Eqs.(7), (8) and (1), it is shown that Eq.(9) has only two independent parameters, u and ϕ_a, and thus can be simplified as follows:

$$\boldsymbol{\varphi}(u,\phi_a)=\boldsymbol{\varphi}(u,\phi_a,\phi_b,\theta)$$
$$=[\chi(u,\phi_a,\phi_b,\theta)\ \ \eta(u,\phi_a,\phi_b,\theta)\ \ \xi(u,\phi_a,\phi_b,\theta)]^{\mathrm{T}}. \tag{10}$$

In the range of $0\le u\le H$,

$$-\arcsin\left(\frac{a-R_b}{R_a}\right)\le\phi_a\le\arcsin\left(\frac{a-R_b}{R_a}\right), \tag{11}$$

where a is the central distance between the star-wheel and the screw rotor; R_a is the radius of the star-wheel; R_b is the radius of the screw rotor.

Meshing surface of the tooth flanks

On the other hand, the contact surface on the envelope column can be obtained by substituting Eq.(7) or (8) into Eq.(3), is expressed as

$$\boldsymbol{c}_2=[\kappa(u,\phi_a)\quad\tau(u,\phi_a)\quad\sigma(u,\phi_a)]^{\mathrm{T}}, \tag{12}$$

where

$$\begin{cases}\kappa(u,\phi_a)=L-u\sin\beta+\dfrac{d}{2}\cos[\theta(u,\phi_a)]\cos\beta,\\ \tau(u,\phi_a)=K+u\cos\beta+\dfrac{d}{2}\cos[\theta(u,\phi_a)]\sin\beta,\\ \sigma(u,\phi_a)=M+\dfrac{d}{2}\sin[\theta(u,\phi_a)].\end{cases}$$

Because there are only two independent parameters in Eq.(12), the equation expressing the contact line can be obtained by giving the value of ϕ_a.

The contact arc marked by the envelope angle, α, as shown in Fig.3, could be easily obtained by subtracting the minimum value of $\theta(u,\phi_a)$ from its maximum value at the given value of u. And the greater the column diameter, d, the longer the length of the contact arc, and thus the better the wear-resistance of the meshing pair and the longer the operating life of SSCs.

The diameter of the envelope column should be equal to that of the milling cutter, because the milling cutter surface fabricates the groove flank as the envelope column moves along the groove flank to obtain good meshing between them. The larger the diameter of the milling cutter, the greater the envelope column diameter. Thus while a large diameter milling cutter is suitable, this diameter must, however, be smaller than that of the groove width. The diameter of the milling cutter, i.e., the column diameter d is thus limited by geometrical and kinematic conditions as follows:

$$d<\frac{(a-R_a)p}{\sqrt{(a-R_a)^2p^2+R_a^{\,2}}}b. \tag{13}$$

DESIGN METHOD FOR CEMP

The diameter of the column, d, and other geometrical parameters of the meshing pair, (L, K, M, H, β), should be determined from the mathematical model of the CEMP. The geometrical parameters are shown in Fig.4 and Fig.5. And other parameters of the compressor, i.e., the thickness of the star-wheel t, the diameters of the screw rotor and the star-wheel, the length and width of the star-wheel tooth, and the centric distance of the meshing pair, could be determined according to the required discharge capacity and compression ratio of the compressor.

Firstly, the inclinational angle of the envelope column β is usually set as 0°. The diameter of the column d is taken as its maximum, as shown in Eq.(13).

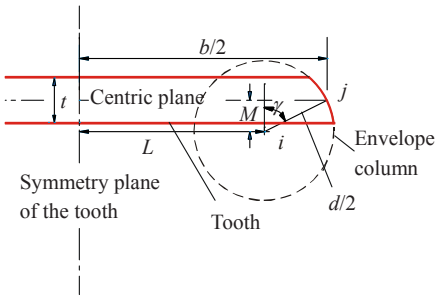

Fig.5 Position of the envelope column at the tooth root

Secondly, the coordinates L, K, and M give the position of the envelope column, denoted by "i" in Fig.4. On the other side, the position of the envelope column at the root of the tooth could be denoted by introducing an angle γ as shown in Fig.5. So the L, K, and M are given by the following equation:

$$\begin{cases} M=-\dfrac{d}{2}\cos\gamma, \\ L=\dfrac{b}{2}-\dfrac{d}{2}\sin\gamma, \\ K=\sqrt{(R_{\mathrm{a}}-l)^2-\left(\dfrac{b}{2}-\dfrac{d}{2}\sin\gamma\right)^2}. \end{cases} \tag{14}$$

The length of the column H is

$$H=l/\cos\beta. \tag{15}$$

Then the design work is focused on the introduced angle γ. Substituting Eq.(14) into Eq.(7), the meshing angle θ is obtained at the position u=0:

$$\theta(\gamma,\phi_{\mathrm{a}})=\operatorname{arctg}\left[\frac{E(\gamma,\phi_{\mathrm{a}})\big|_{u=0}}{F(\gamma,\phi_{\mathrm{a}})\big|_{u=0}}\right], \tag{16}$$

where

$$-\arcsin\left(\frac{a-R_{\mathrm{b}}}{R_{\mathrm{a}}}\right)\le\phi_{\mathrm{a}}\le\arcsin\left(\frac{a-R_{\mathrm{b}}}{R_{\mathrm{a}}}\right). \tag{17}$$

Finally, the meshing angle θ is limited by the tooth thickness t. Here θ ranges to satisfy the condition that the contact surface of the envelope column is within the tooth flank and thus,

$$\frac{\pi}{2}-\arccos\frac{2M-t}{d}\le\theta\le\frac{\pi}{2}-\arccos\frac{2M+t}{d}. \tag{18}$$

The value of γ should be given as an initial condition repeatedly until $\theta(\gamma,\phi_{\mathrm{a}})$ satisfies the above condition.

The CEMP of an SSC with a discharge capacity of 3 m^3/min is designed, and the dimensions are obtained as depicted in Tables 1 and 2.

Table 1 Dimensions of the SSC

Parameter	Value
Radius of star-wheel and rotor, R (mm)	77
Tooth thickness, t (mm)	7
Central distance of the compressor, a (mm)	123.2
Tooth width, b (mm)	23
Tooth length, l (mm)	30.8

Table 2 Design results of the CEMP

Parameter	Value
Diameter of the column, d (mm)	16
Position of the envelope column, L (mm)	4.622
Position of the envelope column, K (mm)	45.968
Position of the envelope column, M (mm)	−4
Height of the envelope column, H (mm)	76.15
Inclinational angle of the envelope column, β (rad)	0
Position angle of the envelope column, γ (rad)	π/3

The envelope angle, α, in Fig.3 is obtained as 0.268 rad when subtracting the minimum from the maximum value of $\theta(u,\phi_{\mathrm{a}})$ at the tooth tip, u=H. And the contact arc at the tooth tip is given as $\alpha d/2$=2.2 mm. It means that the contacting surface of the tooth flank is wide enough to enhance the wear-resistance of the meshing pair.

In addition, the γ denoting the position of the envelope column at the tooth root ranged between 0.826 and 1.14 rad in the above case. However, the area of the sides of the tooth flank exposed to high pressure in the high-pressure chamber and its clearance to the groove flanks would depend on the amount of γ, and thus the gas forces applied on the star-wheel and lubricating situation would also depend on y. So the value of γ must be optimized to balance the gas forces on the star-wheel, and also to improve the lubricating situation.

CONCLUSION

In this paper the mathematical model for CEMP in the SSC is derived from the geometry and kinematics. Research focuses on the geometrical parameters of the CEMP, which enables the design of the compressor by CAD/CAE/CAM.

A design method for the CEMP is proposed based on the mathematical model, and then parameters for the CEMP of an SSC with a discharge capacity of 3 m^3/min are designed. Thus it is shown that the contacting surface of the tooth flank is wide enough to enhance the wear-resistance of the meshing pair.

Results obtained from this paper could be applied in the design and production of the single screw compressor (Sun and Fang, 2006; Kiyoharu, 2007), and thus could accelerate its industrial application.

ACKNOWLEDGEMENTS

The authors wish to express their appreciation to Prof. Takeshi Kawai (School of Energy and Power Engineering, Xi'an Jiaotong University, Xi'an) for his valuable comments on this publication.

References

Bein, T.W., 1991. High Pressure Single Screw Compressors. US Patent No. 4981424.

Boblitt, W.W., 1987. Method for Cutting Complex Tooth Profiles in a Cylindrical, Single-screw Gate-rotor. US Patent No. 4710076.

Jensen, D., 1998. A New Single Screw Compressor Design that Enables a New Manufacturing Process. Compressor Technology Conference, Purdue, p.601-606.

Jensen, D., 2000. Method for Manufacturing Fluid Compression/Compressor Rotor. US Patent No. 6122824.

Jin, G.X., Tang, Y., 1985. Recent advances in the profile study of the engagement pair of a single-screw compressor. *Journal of Xi'an Jiaotong University*, **19**(6):1-9 (in Chinese).

Kang, S.K., Ehmann, K.F., Lin, C., 1996. A CAD approach to helical groove machining—I. Mathematical model and model solution. *International Journal of Machine Tools and Manufacture*, **36**(1):141-153. [doi:10.1016/0890-6955(95)92631-8]

Kiyoharu, Y., 2007. Apparatus and Method for Processing Screw Rotor and Cutting Bit. US Patent No. 7216407.

Liu, Z.M., Hou, D.H., Wang, X.C., Zhang, X.Z., 2000. Computer Aided Analysis and Manufacture for Engagement Pair of Single Screw Compressor. 5th International Conference on Progress of Machining Technology (ICPMT 2000), p.818-823.

Richmond, D., 1996. Methods of grinding spur and helical gears. *Manufacturing Engineering*, **116**(5):87-92.

Sun, X.F., Fang, D.D., 2006. Brand new technology for machining toroid worm of single screw compressor. *Fluid Machinery*, **34**(1):50-52 (in Chinese).

Wu, W.F., Feng, Q.K., Xu, J., 2007. Principle of multi-column envelope couple of single screw compressor. *Journal of Xi'an Jiaotong University*, **41**(11):1271-1274 (in Chinese).

Wu, Z.Y., Tao, G.L., 2005. A Mathematical Model of Movable Component in Single Screw Compressor. Proceedings of the Sixth International Conference on Fluid Power Transmission and Control, p.276-279.

Wu, Z.Y., Tao, G.L., 2006. Simulation of high speed single screw compressor in fuel cell. *Journal of Zhejiang University (Engineering Science)*, **40**(2):309-312, 333 (in Chinese).

Yang, S.C., 2002. A mathematical model of the rotor profile of the single screw compressor. *Proceedings of the Institution of Mechanical Engineers, Part C: Journal of Mechanical Engineering Science*, **216**(3):343-351. [doi:10.1243/0954406021525052]

Yang, S.C., 2006. Profile generation and analysis for a PP-type single-screw compressor. *International Journal of Advanced Manufacturing Technology*, **30**(9-10):789-796. [doi:10.1007/s00170-005-0132-8]

Yang, S.C., Liang, T.L., 2007. Modeling and manufacturing of PP-type single screw compressor. *Transactions of the Canadian Society for Mechanical Engineering*, **31**(2):219-234.

Zhang, S., 2007. The comparison of twin and single screw refrigerating compressor. *Low Temperature and Specialty Gases*, **25**(03):1-4 (in Chinese).

Zhang, S.C., Yu, X.Y., Jin, G.X., 2006. Research of the essential geometric relations of engagement pair for single screw compressor. *Compressor Technology*, **200**(06):21-23 (in Chinese).

Zimmern, B., 1976. Rotary Injection Worm and Worm Wheel with Specific Tooth Shape. US Patent No.3932077.

Zimmern, B., 1990. Method and a Screw Machine for Processing Fluid under High Pressures with Liquid Injection Between a Sealing Portion and a Support Portion of the Gate Rotor. US Patent No. 4900239.

Zimmern, B.., 2000. Single Screw Compressor with Liquid Lock Preventing Slides. US Patent No. 6106241.

Zimmern, B., Ganshyam, Patel, C., 1972. Design and Operating Characteristics of the Zimmern Single Screw Compressor. Compressor Technology Conference, p.96-99.